Journal of Southeast University (English Edition) Vol. 25, No. 4, pp. 486 – 490 Dec. 2009 ISSN 1003—7985

Low-dimensional multi-spectral space for color reproduction based on nonnegative constrained principal component analysis

Wang Ying[1] Zeng Ping[1, 2] Luo Xuemei[1] Xie Kun[1]

([1]School of Computer Science and Technology, Xidian University, Xi'an 710071, China)

([2]School of Computer Science, Xi'an Shiyou University, Xi'an 710065, China)

Abstract: In order to overcome the shortcomings that the reconstructed spectral reflectance may be negative when using the classic principal component analysis (PCA) to reduce the dimensions of the multi-spectral data, a nonnegative constrained principal component analysis method is proposed to construct a low-dimensional multi-spectral space and accomplish the conversion between the new constructed space and the multi-spectral space. First, the reason behind the negative data is analyzed and a nonnegative constraint is imposed on the classic PCA. Then a set of nonnegative linear independence weight vectors of principal components is obtained, by which a low-dimensional space is constructed. Finally, a nonlinear optimization technique is used to determine the projection vectors of the high-dimensional multi-spectral data in the constructed space. Experimental results show that the proposed method can keep the reconstructed spectral data in [0, 1]. The precision of the space created by the proposed method is equivalent to or even higher than that by the PCA.

Key words: spectral color science; nonnegative constrained principal component analysis; low-dimensional spectral space; nonlinear optimization; multi-spectral images; spectral reflectance

Multi-spectral images are those whose pixel values are the spectral reflectance of source scenes. They are mainly used for the accurate and consistent color reproductions of source scenes under different illuminants. Now they have been widely used in high-end imaging fields such as art archiving[1–2], tele-medicine[3–4], and military target imaging.

Multi-spectral images are acquired by narrow-band sampling in the range of visible light, e. g., from 400 to 700 nm. This results in a high dimension of image data. When the images are reproduced by hardcopy devices, high dimension will lead to high computational complexity, large storage space and long computing time during color mapping, device color space transforming and color calibrating. Moreover, because the number of channels of the output devices are far less than the dimension of the image data, the color gamut mapping is almost impossible to be accomplished during color management. Therefore, constructing a low-dimensional space, then transforming the multi-spectral data to it and handling the images in it become the key technologies in multi-spectral image reproduction.

When constructing a low-dimensional space, two principles must be followed. First, the constructed space and the multi-spectral space can be converted to each other. The spectral reflectance reconstructed from the low-dimensional space must have physical significance. That is, it must be in [0, 1]. Secondly, the dimension of the space must be appropriate for the establishment of a look-up table. Creating a look-up table is a common method to solve the computing bottleneck in image reproduction. Whereas the size of the look-up table is exponential to the input dimensions, so the dimension of the constructed space must be fit for establishing and searching in the look-up table.

Several methods have been used to construct the low-dimensional spectral space, including principal component analysis(PCA)[5–6], Karhunen-Loeve transformation[7–8] and LabPQR[9–10]. They are all developed from the PCA theory and can reduce the dimension of spectral data to 6 to 8. Whereas when reconstructing high-dimensional data from the low-dimensional, the data usually exceed the range of [0, 1], which is meaningless because the spectral reflectance is the ratio of the reflected radiant flux to the incident. This leads to the problem that some color management functions cannot be achieved correctly, e. g. image screen proofing. To solve this problem, a nonnegative constrained principal component analysis(NCPCA) method is presented in this paper. It makes the reconstructed spectral reflectance in [0, 1], which holds the physical significance of the spectral reflectance. At the same time it can achieve the precision equivalent to the classic PCA.

1 Principal Component Analysis

The main idea behind the PCA is to project multidimensional data to a low-dimensional space while holding the variance of the source data as great as possible. We assume that $\boldsymbol{S}$ is a $P \times N$ matrix and represents a set of spectral reflectance samples. It has N sample vectors with P dimensions each. The PCA is used to obtain a linear combination $\boldsymbol{C}$ of the source data that makes the variance of $\boldsymbol{C}$ be as great as possible. $\boldsymbol{C}$ is denoted as

$$\boldsymbol{C} = \boldsymbol{a}^{\mathrm{T}}\boldsymbol{S} \tag{1}$$

The variance of $\boldsymbol{C}$ can be described as

$$\mathrm{var}(\boldsymbol{C}) = \mathrm{var}(\boldsymbol{a}^{\mathrm{T}}\boldsymbol{S}) = \boldsymbol{a}^{\mathrm{T}}\boldsymbol{\Sigma}\boldsymbol{a} \tag{2}$$

where $\boldsymbol{\Sigma}$ is the covariance matrix of the source data and is represented as

Received 2009-06-19.

Biographies: Wang Ying (1977—), female, graduate; Zeng Ping (corresponding author), male, professor, zp8637@126.com.

Foundation items: The Pre-Research Foundation of National Ministries and Commissions (No. 9140A16050109DZ01), the Scientific Research Program of the Education Department of Shanxi Province (No. 09JK701).

Citation: Wang Ying, Zeng Ping, Luo Xuemei, et al. Low-dimensional multi-spectral space for color reproduction based on nonnegative constrained principal component analysis[J]. Journal of Southeast University (English Edition), 2009, 25(4): 486 – 490.

$$\boldsymbol{\Sigma} = \frac{1}{P}\boldsymbol{S}\boldsymbol{S}^{\mathrm{T}} \tag{3}$$

By Eq. (2), obtaining the maximum of var($\boldsymbol{C}$) is converted to calculate the maximum of the quadratic form $\boldsymbol{a}^{\mathrm{T}}\boldsymbol{\Sigma}\boldsymbol{a}$. The maximum problem is expressed as

$$\begin{aligned} &\max\ \mathrm{var}(\boldsymbol{C}) = \boldsymbol{a}^{\mathrm{T}}\boldsymbol{\Sigma}\boldsymbol{a} \\ &\text{s. t. } \boldsymbol{a}^{\mathrm{T}}\boldsymbol{a} = 1 \end{aligned} \tag{4}$$

To solve the maximum problem in Eq. (4), the following Lagrange multipliers technique is used,

$$\max\ L(\boldsymbol{a},\ \lambda) = \boldsymbol{a}^{\mathrm{T}}\boldsymbol{\Sigma}\boldsymbol{a} + \lambda(1 - \boldsymbol{a}^{\mathrm{T}}\boldsymbol{a}) \tag{5}$$

We obtain $\frac{\partial}{\partial \boldsymbol{a}}(\boldsymbol{a}^{\mathrm{T}}\boldsymbol{\Sigma}\boldsymbol{a} + \lambda(1 - \boldsymbol{a}^{\mathrm{T}}\boldsymbol{a})) = \boldsymbol{\Sigma}\boldsymbol{a} - \lambda\boldsymbol{a} = 0$, then

$$\boldsymbol{\Sigma}\boldsymbol{a} = \lambda\boldsymbol{a} \tag{6}$$

From Eq. (6) we can see that finding the answer of Eq. (5) is converted to obtain the eigenvalues ($\lambda_1, \lambda_2, \ldots, \lambda_r$) and eigenvectors ($\boldsymbol{a}_1, \boldsymbol{a}_2, \ldots, \boldsymbol{a}_r$) of $\boldsymbol{\Sigma}$, where $\lambda_1 \geqslant \lambda_2 \geqslant \ldots \lambda_r > 0$ are all non-zero eigenvalues of $\boldsymbol{\Sigma}$ and $r = \mathrm{rank}(\boldsymbol{\Sigma})$. Now $\boldsymbol{a}_1$ is the weight vector that makes var($\boldsymbol{C}$) the largest and is defined as the first principal component loading. $\boldsymbol{a}_2$ makes var($\boldsymbol{C}$) the second largest and is defined as the second principal component loading. Followed by analogy, $\boldsymbol{a}_r$ is the r-th principal component loading.

Given $\boldsymbol{V} = [\boldsymbol{a}_1\ \ \boldsymbol{a}_2\ \ \ldots\ \ \boldsymbol{a}_r]$, the multi-spectral data can be projected to the eigenvector space by

$$\boldsymbol{C} = \boldsymbol{V}^{\mathrm{T}}\boldsymbol{S} \tag{7}$$

On the other hand, the multi-spectral data can be reconstructed from the eigenvector space by

$$\hat{\boldsymbol{S}} = \boldsymbol{V}\boldsymbol{C} \tag{8}$$

where $\hat{\boldsymbol{S}}$ is the reconstructed spectra of $\boldsymbol{S}$.

2 Method of Constructing Low-Dimensional Space Using NCPCA

By the analysis of the above PCA theory, the properties using the PCA to reduce the spectral data dimension can be explained as follows:

Property 1 From Eq. (3), we know that $\boldsymbol{\Sigma}$ is a symmetric and nonnegative matrix. All its eigenvalues are nonnegative and the eigenvectors are orthogonal to each other. So there is only one nonnegative eigenvector at most. This leads to the fact that the reconstructed spectra using Eq. (8) cannot always be nonnegative and lose their physical significance.

Property 2 The premise of the conversion between the multi-spectral space and the low-dimensional space using Eq. (7) and Eq. (8) is that transformation matrix $\boldsymbol{V}$ must be orthogonal, that is, $\boldsymbol{V}^{-1} = \boldsymbol{V}^{\mathrm{T}}$.

2.1 Non-negative constrained principal component analysis

To solve the problem caused by using the classic PCA to reduce the spectral data dimension, a nonnegative constraint is imposed on the maximum problem in Eq. (4),

$$\begin{aligned} &\max\ \mathrm{var}(\boldsymbol{C}) = \boldsymbol{a}^{\mathrm{T}}\boldsymbol{\Sigma}\boldsymbol{a} \\ &\text{s. t. } \boldsymbol{a}^{\mathrm{T}}\boldsymbol{a} = 1 \quad \boldsymbol{a} \geqslant \boldsymbol{0} \end{aligned} \tag{9}$$

From the PCA theory, we know that the first principal component should make var($\boldsymbol{C}$) the greatest and represent the most information of the source data. Assuming that $\boldsymbol{a}_1$ is the first principal component loading, the first principal component $\boldsymbol{c}_1$ is obtained by Eq. (1). Hence $\boldsymbol{a}_1\boldsymbol{c}_1$ is the most important approximation of the source spectra. Then

$$\boldsymbol{S}^{(1)} = \boldsymbol{S}^{(0)} - \boldsymbol{a}_1\boldsymbol{c}_1 \tag{10}$$

represents the residual information, where $\boldsymbol{S}^{(0)} = \boldsymbol{S}$ is the source data. Computing the covariance matrix $\boldsymbol{\Sigma}_1$ of $\boldsymbol{S}^{(1)}$ and putting it into Eq. (9), we obtain the first principal component loading $\boldsymbol{a}_2$ of $\boldsymbol{S}^{(1)}$. Then by Eq. (1) we obtain $\boldsymbol{c}_2$. So $\boldsymbol{a}_2\boldsymbol{c}_2$ is the most important approximation of $\boldsymbol{S}^{(1)}$ and is the second approximation of $\boldsymbol{S}^{(0)}$. Repeat the above process, and an iteration is obtained,

$$\boldsymbol{S}^{(t)} = \boldsymbol{S}^{(t-1)} - \boldsymbol{a}_t\boldsymbol{c}_t \tag{11}$$

Using Eq. (11) to calculate $\boldsymbol{S}^{(t)}$ in turn, computing $\boldsymbol{\Sigma}_t$, and then putting them into Eq. (9), we obtain all the principal component loadings of $\boldsymbol{S}$. The most important property of the loadings obtained is that they are all nonnegative.

The solution of the maximum problem in Eq. (9) cannot be converted to solve the eigenvalues and eigenvectors of the covariance matrix because the nonnegative constraint exists. But Eq. (9) is an optimization in itself. It can be solved by a nonlinear optimization. In this paper, the Newton method is utilized.

Through the above process and by r iterations of Eq. (9) and Eq. (10), a set of nonnegative vectors can be obtained. We denote them as $\boldsymbol{V}' = [\boldsymbol{a}_1\ \ \boldsymbol{a}_2\ \ \ldots\ \ \boldsymbol{a}_r]$. Then the best approximation of $\boldsymbol{S}$ is calculated by

$$\hat{\boldsymbol{S}} = \sum_{i=1}^{r} \boldsymbol{a}_i\boldsymbol{c}_i \tag{12}$$

This shows that if using $\boldsymbol{V}'$ as the base vector group, the source data can be expressed as a linear combination of $\boldsymbol{V}'$. Moreover, because $\boldsymbol{V}'$ is a nonnegative vector group, we can obtain the best nonnegative approximation of the source data if the coefficient ($\boldsymbol{c}_1, \boldsymbol{c}_2, \ldots, \boldsymbol{c}_r$) is chosen appropriately. So the following problem is formed,

$$\begin{aligned} &\min\ \varepsilon = \|\boldsymbol{S} - \hat{\boldsymbol{S}}\|_2^2 = \left\|\boldsymbol{S} - \sum_{i=1}^{r} \boldsymbol{a}_i\boldsymbol{c}_i\right\|_2^2 \\ &\text{s. t. } 0 \leqslant \boldsymbol{c}_i \leqslant 1 \end{aligned} \tag{13}$$

Solving the nonlinear optimization in Eq. (13), a set of coefficients ($\boldsymbol{c}_1, \boldsymbol{c}_2, \ldots, \boldsymbol{c}_r$) is obtained. Then putting them into Eq. (12), the approximation $\hat{\boldsymbol{S}}$ of $\boldsymbol{S}$ is obtained. Obviously $\hat{\boldsymbol{S}}$ is nonnegative. Therefore, by using $\boldsymbol{V}'$ to span an r-dimensional space, the conversion from the multi-spectral data to the r-dimensional space is achieved by Eq. (13). On the other hand, given ($\boldsymbol{c}_1, \boldsymbol{c}_2, \ldots, \boldsymbol{c}_r$), high-dimensional spectral data can be reconstructed from the r-dimensional space by Eq. (12). The reconstructed data has the physical significance of the spectral reflectance, and can be used as

the approximation of the source data. During this conversion, $\boldsymbol{V}'$ need not be orthogonal because of the utilization of the nonlinear optimization. So the conversion between the spaces uses Eq. (12) and Eq. (13) instead of Eq. (7) and Eq. (8). In Eq. (9) and Eq. (13), the convergence condition is set as $\| \nabla \mathrm{var}(\boldsymbol{C}) \| < 10^{-4}$, $\| \nabla \boldsymbol{a} \| < 10^{-6}$ and $\| \nabla \boldsymbol{\varepsilon} \| < 10^{-4}$, $\| \nabla \boldsymbol{c} \| < 10^{-6}$ in the experiment. They can be set as other values according to the application.

2.2 Steps of creating low-dimensional space using NCPCA

1) Choose a set of representative spectral samples as the source data;

2) Use Eq. (9) and Eq. (11) to obtain the nonnegative vector group ($\boldsymbol{a}_1$, $\boldsymbol{a}_2$, ..., $\boldsymbol{a}_k$) from the samples in step 1);

3) Exploit the vector group produced by step 2) to construct a k-dimensional space, where k is less than the dimension of the spectral data. The k-dimensional space is the very space that can be served as the fixed low-dimensional space.

4) For any multi-spectral image, its data can be converted to the fixed k-dimensional space by Eq. (13), and its approximation can be reconstructed from the k-dimensional space by Eq. (12).

2.3 Dimension of low-dimensional space

When determining the dimension of the space, two factors should be taken into account. First, the size of the look-up table should be feasible. The relationship of the space dimension and the size of the look-up table are shown in Tab. 1, assuming that the output dimension is six and the output bands are 1 byte each. As shown in Tab. 1, when the input dimension is more than 9, the establishing and searching in a look-up table are almost impossible to achieve.

Tab. 1 Relationship of input dimension and size of look-up table

Input dimension	Sampling numbers in each dimension	Output dimension	Size of look-up table/GB
3	17	6	30×10^{-6}
6	17	6	145×10^{-3}
9	17	6	700
31	17	6	8×10^{29}

Secondly, the data in the low-dimensional space should reflect the information in the source data as much as possible. The variance contribution rates can express the information rates reflected by each principal component. When the accumulative variance contribution rates of the first K principle component reach a certain percentage, the contribution of the K to P principal components can be ignored. The equation of variance contribution rates and accumulative variance contribution rates are as follows:

$$R_k = \lambda'_k / \sum_{i=1}^{P} \lambda'_i \tag{14}$$

$$R = \sum_{k=1}^{K} \lambda'_k / \sum_{i=1}^{P} \lambda'_i \tag{15}$$

where λ'_i is the variance calculated by Eq. (9).

3 Experiments

In the experiment, the spectral reflectance of the color patch IT8.7/3 is utilized as the base samples. IT8.7/3 is a standard print target and commonly used in color print reproduction experiments. It has 928 color samples. The nonnegative vector group is produced by these samples and is utilized to construct the low-dimensional space. The spectral reflectance of the base samples is sampled from 400 to 700 nm at 10 nm intervals. The dimension of the data is 31. Tab. 2 shows the variance contribution rates using the classic PCA and NCPCA respectively to reduce the dimension of the base samples. As shown in Tab. 2, for the same numbers of the principal components, although the represented information using PCA is slightly larger than using NCPCA, the accumulative variance contribution rates using NCPCA still reach a high level.

By the analysis of Tab. 1 and Tab. 2, the six-dimensional space is chosen as the low-dimensional space. The look-up table based on this space is appropriate in size and favorable in storage and search. Moreover, the accumulative variance contribution rates of the first six principal components reach 99%. So they can represent the information of the source data well.

Tab. 2 Variance contribution rates using classic PCA and NCPCA

Method	Variable	c_1	c_2	c_3	c_4	c_5	c_6	c_7	c_8	c_9
PCA	Variance	1.079 2	0.245 6	0.118 1	0.014 8	0.003 9	0.002 7	0.001 3	0.000 8	0.000 1
	VCR	0.735 9	0.167 4	0.080 5	0.010 1	0.002 7	0.001 8	0.000 8	0.000 5	0.000 1
	AVCR	0.735 9	0.903 3	0.983 8	0.993 9	0.996 6	0.998 4	0.999 2	0.999 7	0.999 8
NCPCA	Variance	1.079 2	0.139 0	0.122 1	0.097 2	0.008 4	0.008 1	0.004 3	0.002 2	0.001 9
	VCR	0.736 6	0.094 9	0.083 3	0.066 3	0.005 7	0.005 6	0.003 0	0.001 5	0.000 8
	AVCR	0.736 6	0.831 5	0.914 8	0.981 1	0.986 8	0.992 4	0.995 4	0.996 9	0.997 7

Note: VCR means variance contribution rates and AVCR means accumulative variance contribution rates.

The six-dimensional space is constructed by the PCA and the NCPCA, respectively. The spectral reflectance of IT8.7/3 is reconstructed from the space. Their curves are shown in Fig. 1. From Fig. 1 we can see that negative data appear using the PCA. This results in meaningless spectra. Yet the data produced by the NCPCA is in [0, 1]. They can be used as the approximation of the source spectra. Tab. 3 shows the precision of the low-dimensional space constructed by two methods, where the normalized PCA means that the reconstructed data using the PCA is normalized in [0, 1]. The spectral precision is evaluated by the root mean square error E_{RMS} [11], and the colorimetric precision by the standard CIELAB color difference equation ΔE_{ab} under a typical illuminant. From Tab. 3 we know the precision using the PCA is slightly higher than using the NCPCA when the dimension of the space is the same. This is caused by the fact that the eigenvectors of the PCA are orthogonal and that of the NCPCA are only linearly inde-

pendent. In addition, the process of the PCA is linear, yet the NCPCA is affected by the convergence precision of the optimization. Nevertheless, the precision of the PCA and the NCPCA is very close. This shows that the NCPCA can be used as a low-dimensional space construction method.

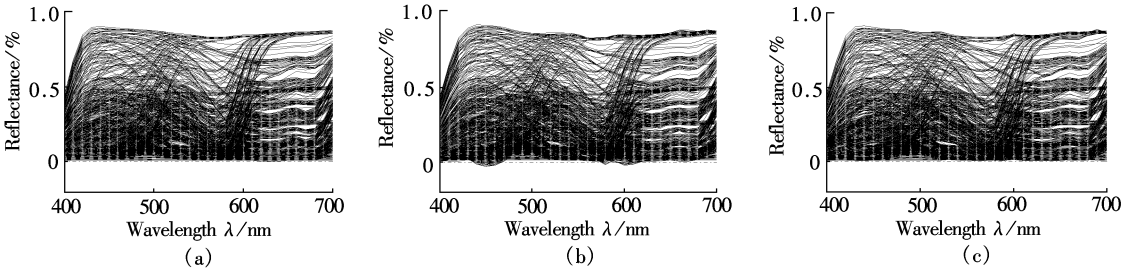

Fig. 1 Spectral reflectance curve of IT8. 7/3. (a) Source data; (b) Reconstructed data using PCA; (c) Reconstructed data using NCPCA

Tab. 3 Precision of the low dimensional space using the three methods

Method	ΔE_{ab} (D65, 2° observer)				E_{RMS}			
	Mean	Standard deviation	Min	Max	Mean	Standard deviation	Min	Max
PCA	0. 120 2	0. 132 7	0. 000 6	0. 975 9	0. 002 4	0. 001 1	0. 000 7	0. 006 8
PCA(normalized)	0. 697 8	0. 664 9	0. 025 8	4. 227 3	0. 003 6	0. 001 6	0. 000 9	0. 016 5
NCPCA	0. 151 8	0. 211 8	0. 000 8	1. 237 7	0. 002 6	0. 002 2	0. 000 5	0. 010 3

Two multi-spectral images are used as the test images. They are converted to the space constructed by the samples of IT8. 7/3, and then reconstructed from the space. Both the images are sampled in 400 to 700 nm at 10 nm intervals. The RGB images synthesized from the multi-spectral images are shown in Fig. 2. Fig. 2 (a) is a typical skin image and Fig. 2(b) is a scene picture with high color saturation. Tab. 4 shows the conversion precision of the two images.

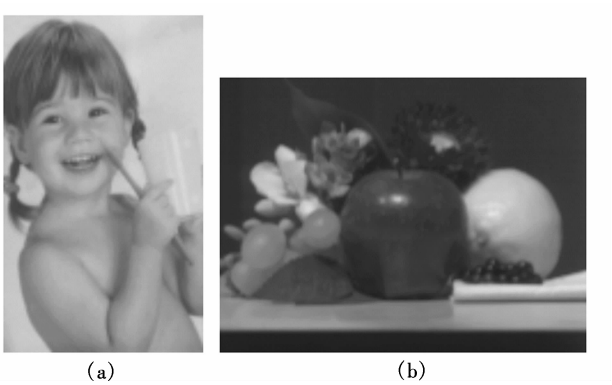

Fig. 2 RGB images synthesized from multi-spectral images. (a) Young-girl; (b) Fruits-and-flowers

Tab. 4 Conversion precision of the two images using the two methods

Image	Method	ΔE_{ab} (D65, 2° observer)		E_{RMS}	
		Mean	Standard deviation	Mean	Standard deviation
Fig. 2(a)	PCA	0. 119 9	0. 062 9	0. 010 4	0. 007 8
	NCPCA	0. 078 9	0. 062 0	0. 003 2	0. 000 9
Fig. 2(b)	PCA	1. 329 9	1. 307 4	0. 016 9	0. 007 7
	NCPCA	1. 586 3	1. 217 5	0. 010 7	0. 008 6

As shown in Tab. 4, the NCPCA can reach the close precision of the classic PCA. Sometimes the accuracy is even higher than that of the PCA. Since the image of fruits-and-flowers has a large amount of color with high saturation and the color exceeds the gamut of the IT8. 7/3, its precision is lower than that of the young-girl. This shows that choosing appropriate base samples to construct the low-dimensional space is crucial for improving the accuracy of the space conversion.

4 Conclusion

An NCPCA method is presented in this paper aiming at constructing a low-dimensional space. By imposing a nonnegative constraint on the classic PCA, it can limit the reconstructed data into the range of [0, 1]. By using a nonlinear optimization, it can obtain the transformation matrix between the high and low dimension spaces. Experiments show that the proposed method not only holds the physical significance of spectral reflectance, but also has a close accuracy with the classic PCA. Moreover, the idea of the NCPCA can be applied to the occasions of dimension reduction and feature extraction where the analysis results need to be nonnegative. How to choose reasonable base spectral samples needs further investigation.

References

[1] Zhao Yonghui, Berns S R, Taplin A L, et al. An investigation of multispectral imaging for the mapping of pigments in paintings[C]//*Proceedings of International Society for Optical and Photonics Engineering*. San Jose, CA, USA, 2008, **6810**: 681007-1-9.

[2] Bochko V, Tsumura N, Miyake Y. A spectral color imaging system for estimating spectral reflectance of paint[J]. *Journal of Imaging Science and Technology*, 2007, **51**(1): 70 - 78.

[3] Munzenmayer C, Paulus D, Wittenberg T. A spectral color correction framework for medical applications[J]. *IEEE Trans on Biomedical Engineering*, 2006, **53**(2): 254 - 265.

[4] Tsummura N, Miyake Y, Imai H F. Medical vision: measurement of skin absolute spectral-reflectance-image and the application to component analysis[C]//*Proceedings of the 3rd Int Conf on Multispectral Color Science*. Joensuu, Finland, 2001: 25 - 28.

[5] Wu Chungyi, Lee Shunming, Wen Chaohua, et al. Multispectral image acquisition system for color spectrum reproduction[C]//*Proceedings of the 16th IPPR Conf on Com-*

puter Vision, Graphics and Image Processing. Kinmen, Taiwan, China, 2003: 115 - 122.
[6] Bakke M A, Farup I, Hardeberg Y J. Multispectral gamut mapping and visualization—a first attempt[C]//*Proceedings of International Society for Optical and Photonics Engineering*. San Jose, CA, USA, 2005, **5667**: 193 - 200.
[7] Yu Shanshan, Murakami Y, Obi T, et al. Multispectral image compression for improvement of colorimetric and spectral reproducibility by nonlinear spectral transform[J]. *Optical Review*, 2006, **13**(2): 346 - 356.
[8] Yu Shanshan, Murakami Y, Obi T, et al. Improvements for multispectral image compression for color reproducibility with preservation to spectral accuracy[C]//*IEEE Int Conf on Image Processing*. Genova, Italy, 2005: 710 - 713.
[9] Derhak W M, Rosen R M. Spectral colorimetry using Lab-PQR: an interim connection space[J]. *Journal of Imaging Science and Technology*, 2006, **50**(1): 53 - 63.
[10] Tsutsumi S, Rosen R M, Berns S R. Spectral color management using interim connection spaces based on spectral decomposition[C]//*Proceedings of the* 14*th Color Imaging Conf*. Arizona, USA, 2006: 246 - 251.
[11] Imai H F, Rosen R M, Berns S R. Comparative study of metrics for spectral match quality[C]//*Proceedings of the First European Conference on Color Graphics, Imaging, and Vision*. Poitiers, France, 2002: 492 - 496.

基于非负主成分分析的低维光谱色彩空间表示法

王 莹[1] 曾 平[1,2] 罗雪梅[1] 谢 琨[1]

([1] 西安电子科技大学计算机学院, 西安 710071)
([2] 西安石油大学计算机学院, 西安 710065)

摘要: 针对采用主成分分析法进行多光谱数据降维会使重构光谱反射比出现负值的问题, 提出一种非负约束主成分分析法, 并用该法构造低维空间, 实现高维多光谱数据向低维空间的转换. 首先分析主成分分析法产生非光谱数据的原因, 据此对经典主成分分析模型增加非负约束; 然后求出一组线性无关的非负主成分权向量, 用该组向量构造低维空间; 最后用非线性优化技术确定高维数据在该低维空间中的投影值, 实现了高维空间与低维空间的相互转换. 实验结果表明, 新方法能使重构光谱数据在[0, 1]内, 保持了光谱反射比的物理意义, 同时所构造低维空间的精度能与经典主成分分析法保持一致.

关键词: 光谱色彩学; 非负约束主成分分析; 低维光谱空间; 非线性优化; 多光谱图像; 光谱反射比
中图分类号: TN911.74; TP301.6